Inorg. Chem. **2008**, *47*, 497–507

Synthesis and Structural and Magnetic Characterization of Cobalt(II) Phosphonate Cage Compounds

Stuart Langley,[†] Madeleine Helliwell,[†] Roberta Sessoli,[‡] Simon J. Teat,[§] and Richard E. P. Winpenny*[,†]

School of Chemistry, The University of Manchester, Oxford Road, Manchester M13 9PL, U.K., Laboratorio di Magnetismo Molecolare, Dipartimento di Chimica, Università degli Studi di Firenze, Polo Scientifico Universitario, Via Lastruccia n. 3, 50019 Sesto Fiorentino, Italy, and CCLRC Daresbury Laboratory, Warrington, Cheshire WA4 4AD, U.K.

Received May 21, 2007

Reaction of cobalt salts with phosphonic acids in the presence of 6-chloro-2-hydroxypyridine as a co-ligand, normally in its deprotonated form, leads to a series of new polymetallic cobalt cages. The most common structural type is a $\{Co_{14}\}$ cage which resembles a fragment of cobalt hydroxide. Variation of the phosphonate present and the cobalt salt leads to $\{Co_6\}$, $\{Co_8\}$, $\{Co_{10}\}$, $\{Co_{11}\}$, $\{Co_{12}\}$, $\{Co_{13}\}$, and $\{Co_{20}\}$ cages, all of which have been characterized by X-ray crystallography. Magnetic studies of these cages show a general decline in the product $\chi_m T$ with T, but for $\{Co_6\}$, $\{Co_8\}$, and $\{Co_{12}\}$ there are maxima at low temperature, which suggests nondiamagnetic ground states. Investigation of the dynamic behavior of the magnetization of these complexes shows that the octanuclear cage displays slow relaxation of magnetization.

Introduction

The synthesis of cage compounds containing paramagnetic ions continues to be a subject pursued by many groups worldwide.[1] The range of ligands used is perhaps a little more limited than one might expect. Carboxylates are almost ubiquitous,[2] pyridonates have been exploited at some length,[3] derivatives of dipyridylketone are common,[4] and alkoxides are found as a co-ligand with all of the above. The justification for these studies derives from the unusual magnetic properties displayed by some of these compounds. The slow relaxation of magnetization first observed in a dodecanuclear heterovalent manganese cluster[5] and later in many other Mn(III) clusters,[6] Fe(III) clusters,[7] a single V(III) cage,[8] and more recently for Ni(II) complexes[9] suggests that magnetic information could be stored in a single molecule, which is appealing. The slow relaxation derives from a high-spin ground state and significant magnetic anisotropy of that ground state.[5−10]

Phosphonates (RPO_3^{2-}) are a family of ligands that should be ideal for stabilizing polymetallic complexes, in that they possess three donor O atoms and could in principle bind to up to nine metal centers. However, the very low solubility of metal phosphonates causes problems with isolation and characterization of such complexes. Three strategies have been adopted to overcome this problem and produce molecular species. Zubieta and co-workers have used solvo-

* To whom correspondence should be addressed. E-mail: richard.winpenny@manchester.ac.uk. Fax: +44-161-275-4598.
[†] The University of Manchester.
[‡] Università degli Studi di Firenze, Polo Scientifico Universitario.
[§] CCLRC Daresbury Laboratory.

(1) (a) Winpenny, R. E. P. *Comp. Coord. Chem. II* **2004**, *7*, 125−176 and references therein.
(2) For example: Aromi, G.; Aubin, S. M.; Bolcar, M. A.; Christou, G.; Eppley, H. J.; Folting, K.; Hendrickson, D. N.; Huffman, J. C.; Squire, R. C.; Tsai, H. L.; Wang, S.; Wemple, M. *Polyhedron* **1998**, *17*, 3005−3020.
(3) Winpenny, R. E. P. *Dalton Trans.* **2002**, 1−10.
(4) For example: Tsohos, A.; Dionyssopoulou, S.; Raptopoulou, C. P.; Terzis, A.; Bakalbassis, E. G.; Perlepes, S. P. *Angew. Chem., Int. Ed.* **1999**, *38*, 983−985.
(5) (a) Sessoli, R.; Tsai, H.-L.; Schake, A. R.; Wang, S.; Vincent, J. B.; Folting, K.; Gatteschi, D.; Christou, G.; Hendrickson, D. N. *J. Am. Chem. Soc.* **1993**, *115*, 1804−1816. (b) Sessoli, R.; Gatteschi, D.; Caneschi, A.; Novak, M. A. *Nature* **1993**, *365*, 141−143.
(6) Aromi, G.; Brechin, E. K. *Struct. Bonding* **2006**, *122*, 1−68.
(7) Gatteschi, D.; Sessoli, R. *Angew. Chem., Int. Ed.* **2003**, *42*, 268−297 and references therein.
(8) Castro, S. L.; Sun, Z. M.; Grant, C. M.; Bollinger, J. C.; Hendrickson, D. N.; Christou, G. *J. Am. Chem. Soc.* **1998**, *120*, 2365−2375.
(9) (a) Andres, H.; Basler, R.; Blake, A. J.; Brechin, E. K.; Cadiou, C.; Chaboussant, G.; Grant, C. M.; Güdel, H.-U.; Harris, S. G.; Murrie, M.; Parsons, S.; Paulsen, C.; Semadini, F.; Villar, V.; Wernsdorfer; W.; Winpenny, R. E. P. *Chem.—Eur. J.* **2002**, *8*, 4867−4876. (b) Murrie, M.; Stöeckli-Evans, H.; Güdel, H. U. *Angew. Chem., Int. Ed.* **2001**, *40*, 1957−1960. (c) Edwards, R. S.; Maccagnano, S.; Yang, E. C.; Hill, S.; Wernsdorfer, W.; Hendrickson, D.; Christou, G. *J. Appl. Phys.* **2003**, *93*, 7807−7809.
(10) Gatteschi, D.; Sessoli, R.; Villain, J. *Molecular Nanomagnets*; Oxford University Press: Oxford, U.K., 2006.

10.1021/ic700984r CCC: $40.75
Published on Web 12/13/2007

thermal techniques to produce a range of vanadium cages.[11] More recently, the Chandrasekhar group has pioneered the concept of using a "co-ligand" to maintain some solubility and has thus made complexes including a dodecanuclear copper complex by including pyrazole as a ligand as well as phosphonate.[12] We have looked at linking preformed cages by displacing carboxylates by phosphonates and have generated a series of iron−carboxylate−phosphonate cages, ranging from tetranuclear to tetradecanuclear.[13] Similarly reactions of phosphonates with oxo-centered manganese carboxylate triangles have led to cages as large as $\{Mn_{20}\}$, some of which show slow relaxation of magnetization.[14] Clearfield and co-workers have published related work on Fe phosphonate cages.[15]

For creating complexes with unusual magnetic properties, phosphonates have advantages and disadvantages. The chief advantage is that they can induce two-dimensional (2D) lattices in extended structures;[16] if the growth of cage compounds can be stopped before 2D materials form, this would be ideal for generating *structural* anisotropy. This may help in generating magnetic anisotropy. The disadvantage is that magnetic exchange via phosphonates is known to be weak; however, the likelihood is that co-ligands (oxide, hydroxide, alkoxides) will also be present, and significant superexchange can be expected through these co-ligands.

Here, we report the synthesis and study of cobalt(II) complexes with phosphonate ligands, using an approach related to that used by Chandrasekhar and co-workers.[12] The resulting complexes show a remarkable range of structural types, none of which could have been predicted, and many of which are difficult to rationalize. The difficulty in modeling the magnetic behavior of Co(II) complexes is well-known, even for dinuclear species; however, we feel it is worth reporting this data, as the existence of such data and further examples of slow relaxation of magnetization in Co(II) compounds may inspire new approaches to modeling the magnetism of complexes of this ion. A preliminary report concerning the $\{Co_8\}$ cluster has been published.[17]

Experimental Section

Preparation of Compounds. All reagents, metal salts, and ligands were used as obtained from Aldrich.

Synthesis of $[Co_{14}(OH)_2(X)_2(chp)_{20}(O_3PR)_2(H_2O)_2]$ (X = F or OH and R = Benzyl, 1; Me, 2; Et, 3; *n*-octyl, 4) and $[Co_{14}(chp)_{20}(Hchp)_2(RPO_3)_2(OH)_2(F)_2(H_2O)_2]$ when R = H, 5). Cobalt perchlorate hexahydrate for **1** and **3** (0.73 g, 2.0 mmol) and cobalt tetrafluoroborate hexahydrate for **2**, **4**, and **5** (0.68 g, 2.0 mmol) were dissolved in acetonitrile (25 mL). To this was added 6-chloro-2-hydroxypyridine (Hchp, 0.52 g, 4.0 mmol), RPO_3H_2 (0.33 mmol) and triethylamine (0.64 mL, 4.7 mmol); this resulted in a deep-purple solution, which was stirred for 6 h. The solution was then filtered, and the solvent was removed to give a purple oil. Extraction with CH_2Cl_2 followed by layering with hexane gave deep-purple crystals. Yields (based on metal): **1**, 22%; **2**, 28%; **3**, 12%; **4**, 17%; **5**, 23%. Elemental Anal. Calcd for $Co_{14}C_{114}H_{82}N_{20}O_{32}P_2Cl_{20}$: C 35.66, H 2.15, N 7.29. Found: C 35.68, H 2.42, N 7.08 for **1**.

Elemental Anal. Calcd for $Co_{14}C_{102}H_{72}N_{20}O_{30}P_2Cl_{20}F_2$: C 33.17, H 1.95, N 7.59. Found: C 32.97, H 1.80, N 7.10 for **2**.

Elemental Anal. Calcd for $Co_{14}C_{110}H_{92}N_{20}O_{32}P_2Cl_{20}$ (**3**·C_6H_{14}): C 34.11, H 2.39, N 7.23: found C 34.68, H 2.42, N 7.40 for **3**.

Elemental Anal. Calcd for $Co_{14}C_{116}H_{100}N_{20}O_{30}P_2Cl_{20}F_2$: C 35.80, H 2.57, N 7.20. Found: C 36.34, H 3.10, N 6.99 for **4**.

Elemental Anal. Calcd for $Co_{14}C_{118}H_{94}N_{22}O_{32}P_2Cl_{26}F_2$ (**5**·$2CH_2Cl_2$·C_6H_{14}): C 33.92, H 2.27, N 7.38. Found: C 33.29, H 2.98, N 7.04 for **5**.

Synthesis of $[Co_{11}(F)(chp)_{18}(PO_4)]$ (6). Synthesis as in **2**, except that FPO_3H_2 (0.033 g, 0.33 mmol) was used in place of RPO_3H_2. Yield: 25%. Elemental Anal. Calcd for $Co_{11}C_{90}H_{54}N_{18}O_{22}PCl_{18}F$: C 35.14, H 1.77, N 8.20, F 0.62. Found: C 35.06, H 1.81, N 8.21, F 1.06.

Synthesis of $[Co_{11}(OH)(chp)_{18}(PO_4)]$ (7). Synthesis as in **6**, except that H_3PO_4 (0.033 g, 0.33 mmol) or $H_2O_3POPO_3H_2$ (0.058 g, 0.33 mmol) was used in place of FPO_3H_2. Yield: 23%. Elemental Anal. Calcd for $Co_{11}C_{91}H_{57}N_{18}O_{23}PCl_{20}$ (**7**·CH_2Cl_2): C 34.60, H 1.82, N 7.98. Found: C 34.32, H 1.93, N 7.95.

Synthesis of $[Co_{12}(OH)_2(chp)_{18}(O_3PCH_2Nap)(HBO_3)(H_2O)]$ (8). Synthesis as in **2**, except that $NapCH_2PO_3H_2$ (0.074 g, 0.33 mmol) was used in place of RPO_3H_2. Yield: 21%. Elemental Anal. Calcd for $Co_{12}C_{108}H_{84}N_{18}O_{27}PCl_{20}B$ (**8**·CH_2Cl_2·C_6H_{14}): C 36.81, H 2.40, N 7.16. Found: C 36.28, H 4.14, N 7.00.

Synthesis of $[Co_{13}(OH)_3(chp)_{19}(O_3PPh)_2(H_2O)_2(EtOAc)_2]$ (9). Synthesis as in **1**, except that $PhPO_3H_2$ (0.052 g, 0.33 mmol) was used in place of RPO_3H_2 and EtOAc was used for extraction and recrystallization in place of CH_2Cl_2. Yield: 25%. Elemental Anal. Calcd for $Co_{13}C_{119}H_{98}N_{19}O_{36}P_2Cl_{19}$: C 36.92, H 2.55, N 6.87. Found: C 36.90, H 2.35, N 6.77.

Synthesis of $[HNEt_3][Co_8(chp)_{10}(O_3PPh)_2(NO_3)_3(Hchp)_2]$ (10). Synthesis as in **2**, except that cobalt nitrate hexahydrate (0.58 g, 2 mmol) and $PhPO_3H_2$ (0.052 g, 0.33 mmol) were used in place of hydrated cobalt tetrafluoroborate and RPO_3H_2, respectively. Yield: 15%. Elemental Anal. Calcd for $Co_8C_{78}H_{64}N_{16}O_{27}P_2Cl_{12}$: C 35.84, H 2.47, N 8.57. Found: C 35.65, H 2.49, N 8.52.

Synthesis of $[Co_{20}(O)_2(OH)_4(chp)_{26}(PhPO_3)_4(H_2O)_6]$ (11). Synthesis as in **10**, except that 4 drops of H_2O_2 (30% soln) was also added to the reaction, giving a deep-brown solution, which was stirred for 6 h. The solution was then filtered, and the solvent was removed to give a brown oil. Extraction with CH_2Cl_2 followed by layering with hexane gave deep-purple crystals. Yield: 20%. Elemental Anal. Calcd for $Co_{20}C_{154}H_{116}N_{26}O_{52}P_4Cl_{26}$: C 34.33, H 2.17, N 6.76. Found: C 34.35, H 2.51, N 7.12.

Synthesis of $[Co_6(chp)_8(O_3P^tBu)_2(Hchp)_2(H_2O)_2]$ (12). Synthesis as for **10**, except $^tBuPO_3H_2$ (0.046 g, 0.33 mmol) was used in place of $PhPO_3H_2$. Yield: 20%. Elemental Anal. Calcd for $Co_6C_{58}H_{54}N_{10}O_{18}P_2Cl_{10}$: C 35.74, H 2.79, N 7.18. Found: C 35.22, H 2.85, N 7.21.

Synthesis of $[Co_{10}(OH)_2(chp)_{14}(O_3PCH_2CH_2PO_3)]$ (13). Synthesis as for **2**, except that $H_2PO_3CH_2CH_2PO_3H_2$ (0.063 g, 0.33 mmol) was used in place of RPO_3H_2. Yield: 38%. Elemental Anal.

(11) Khan, M. I.; Zubieta, J. *Prog. Inorg. Chem.* **1995**, *43*, 1−149 and references therein.
(12) Chandrasekhar, V.; Kingsley, S. *Angew. Chem.* **2000**, *112*, 2410−2412. Chandrasekhar, V.; Kingsley, S. *Angew. Chem., Int. Ed.* **2000**, *39*, 2320−2322.
(13) Helliwell, M.; Langley, S.; Raftery, J.; Tolis, E. I.; Winpenny, R. E. P. *Angew. Chem., Int. Ed.* **2003**, *42*, 3804−3808.
(14) (a) Maheswaran, S.; Chastanet, G.; Teat, S. J.; Mallah, T.; Sessoli, R.; Wernsdorfer, W.; Winpenny, R. E. P. *Angew. Chem., Int Ed.* **2005**, *44*, 5044−5048. (b) Shanmugam, M.; Chastanet, G.; Mallah, T.; Sessoli, R.; Teat, S. J.; Timco, G. A.; Winpenny, R. E. P. *Chem.−Eur. J.* **2006**, *12*, 8777−8785.
(15) Konar, S.; Bhuvanesh, N.; Clearfield, A. *J. Am. Chem. Soc.* **2006**, *128*, 9604−9605.
(16) Clearfield, A. *Curr. Opin. Solid State Mater. Sci.* **1996**, *1*, 268−278.
(17) Langley, S. J.; Helliwell, M.; Sessoli, R.; Rosa, P.; Wernsdorfer, W.; Winpenny, R. E. P. *Chem. Commun.* **2005**, 5029−5031.

Table 1. Crystal Data and Refinement Parameters for **1**−**13**

compound	**1**	**2**	**3**	**4**	**5**
formula	$C_{130}H_{114}Cl_{20}Co_{14}N_{20}O_{38}P_2$	$C_{106}H_{77.50}Cl_{27.50}Co_{14}F_2N_{20}O_{30}P_2$	$C_{104}H_{72}Cl_{20}Co_{14}N_{20}O_{32}P_2$	$C_{120}H_{106}Cl_{28}Co_{14}F_2N_{20}O_{30}P_2$	$C_{123}H_{96}Cl_{32}Co_{14}F_2N_{22}O_{34}P_2$
M	4160.37	4011.21	3709.78	4225.81	4485.58
cryst syst	triclinic	triclinic	triclinic	monoclinic	monoclinic
space group	$P\bar{1}$	$P\bar{1}$	$P\bar{1}$	$P2_1/n$	$C2/c$
a/Å	15.050(4)	15.9493(15)	11.5057(9)	17.517(2)	37.055(3)
b/Å	19.226(4)	21.1635(19)	17.0104(13)	15.2534(17)	15.2124(10)
c/Å	29.599(7)	24.6465(19)	18.4961(14)	29.011(3)	29.2421(18)
α/deg	93.274(5)	68.671(8)	72.361(2)	90	90
β/deg	102.907(5)	85.598(7)	75.564(2)	96.422(2)	97.267(2)
γ/deg	107.484(4)	75.932(8)	88.622(2)	90	90
U/Å^3	7891(3)	7516.4(11)	3335.7(4)	7702.9(15)	16351(2)
T/K	100(2)	100(2)	150(2)	100(2)	100(2)
Z	2	2	1	2	4
μ/mm^{-1}	1.751	1.772	1.847	1.822	1.822
unique data	27 280	26 449	17 417	15 760	14 399
data with $F_o > 4\sigma(F_o)$	11 845	17 819	14 634	13 438	11 284
R1, wR2[a]	0.0684, 0.1637	0.0854, 0.2662	0.0347, 0.0921	0.0399, 0.1137	0.0452, 0.1149

compound	**6**	**7**	**8**	**9**
formula	$C_{92}H_{59}Cl_{22}Co_{11}FN_{18}O_{22.50}P$	$C_{92.50}H_{59}Cl_{23}Co_{11}N_{18}O_{23}P$	$C_{112.50}H_{92}BCl_{25}Co_{12}N_{18}O_{29}P$	$C_{119}H_{67}Cl_{19}Co_{13}N_{19}O_{37}P_2$
M	3254.67	3285.13	3795.23	3856.50
cryst syst	orthorhombic	orthorhombic	monoclinic	triclinic
space group	*Pbca*	*Pbca*	$C2/c$	$P\bar{1}$
a/Å	23.592(2)	24.015(2)	26.1281(17)	16.7557(11)
b/Å	21.203(2)	21.140(2)	21.0494(17)	17.7537(11)
c/Å	46.294(4)	46.308(5)	54.181(4)	29.7580(19)
α/deg	90	90	90	104.1630(10)
β/deg	90	90	101.940(2)	102.6740(10)
γ/deg	90	90	90	94.1470(10)
U/Å^3	23157(4)	23509(4)	29154(4)	8299.4(9)
T/K	100(2)	100(2)	100(2)	100(2)
Z	8	8	8	2
μ/mm^{-1}	1.867	1.856	1.729	1.543
unique data	23 690	20 748	29 769	33 405
data with $F_o > 4\sigma(F_o)$	18 429	9983	24 069	15 205
R1, wR2[a]	0.0472, 0.1101	0.0486, 0.1006	0.0567, 0.1463	0.0795, 0.2566

compound	**10**	**11**	**12**	**13**
formula	$C_{82}H_{69}Cl_{20}Co_8N_{16}O_{27}P_2$	$C_{177}H_{152}Cl_{40}Co_{20}N_{26}O_{56}P_4$	$C_{70}H_{82}Cl_{10}Co_6N_{10}O_{19}P_2$	$C_{76.50}H_{55}Cl_{23}Co_{10}N_{14}O_{22}P_2$
M	2952.91	6259.73	2137.48	2988.94
cryst syst	monoclinic	triclinic	triclinic	monoclinic
space group	$P2_1/n$	$P\bar{1}$	$P\bar{1}$	$C2/c$
a/Å	20.551(2)	16.355(3)	12.0991(13)	18.949(2)
b/Å	21.853(2)	19.214(4)	14.1404(16)	38.092(4)
c/Å	25.909(3)	20.824(4)	14.6073(16)	17.069(2)
α/deg	90	79.698(4)	71.635(2)	90
β/deg	104.703(2)	80.664(4)	72.038(2)	117.298(9)
γ/deg	90	76.032(4)	71.306(2)	90
U/Å^3	11255(2)	6199(2)	2186.1(4)	10948(2)
T/K	100(2)	100(2)	100(2)	100(2)
Z	4	1	1	4
μ/mm^{-1}	1.743	1.677	1.525	1.813
unique data	22 837	17 781	8672	9666
data with $F_o > 4\sigma(F_o)$	10 571	7809	7140	5204
R1, wR2[a]	0.0554, 0.1479	0.0691, 0.1949	0.0456, 0.1307	0.0876, 0.2207

[a] R1 reported for data with $F_o > 4\sigma(F_o)$, wR2 reported for all data.

Calcd for $Co_{10}C_{72}H_{48}N_{14}O_{22}P_2Cl_{14}$: C 33.14, H 1.85, N 7.50. Found: C 32.93, H 2.51, N 7.14.

Structure Determinations. Data for **1** and **4**−**13** were collected on a Bruker SMART CCD diffractometer, data for **2** were collected on an Oxford Instruments CCD diffractometer (Mo Kα, λ = 0.71069 Å), and data for **3** were collected on a Bruker SMART CCD diffractometer using synchrotron radiation (λ = 0.6892 Å). Crystal data and refinement parameters are given in Table 1. In all cases the selected crystals were mounted on the tip of a glass pin using Paratone-N oil and placed in the cold flow (120 K) produced with an Oxford Cryocooling device.[18] Complete hemispheres of data were collected using ω scans (0.3°, 30 s/frame). Integrated intensities were obtained with *SAINT*+,[19] and they were corrected for absorption using *SADABS*.[19] Structure solution and refinement was performed with the *SHELX* package.[19] The structures were solved by direct methods and completed by iterative cycles of ΔF syntheses and full-matrix least-squares refinement against F^2.

(18) Cosier, J.; Glazer, A. M. *J. Appl. Crystallogr.* **1986**, *19*, 105−107.
(19) *SHELX-PC* package; Bruker Analytical X-ray Systems: Madison, WI, 1998.

Magnetic Measurements. The magnetic properties of polycrystalline samples were investigated using a Cryogenic M600 SQUID magnetometer and a home-developed ac probe based on the Oxford Inst. MAGLAB platform.[20]

Results

The synthetic approach adopted has two distinct steps. In the first, the reagents are mixed in a polar solvent—in this case MeCN—keeping the ratio of phosphonic acid/cobalt low—typically 1:6—and including a second ligand to retain the reagents in solution. Here, 6-chloro-2-hydroxypyridine (Hchp) has been used as the co-ligand. A base is added to deprotonate the phosphonic acid and Hchp. The base used has a large influence on the structure; the results reported here use NEt_3. Where NaOMe or LiOMe are used, the resulting cage complexes incorporate the alkali-metal cation.[21] The solution is then evaporated to dryness, giving a paste or oil. The second step is to extract this paste with a range of solvents. Crystallization is achieved from these solutions either directly or by adding a solvent of lower polarity, typically by layering with hexanes. We can only be certain that the product is present in the crystalline material obtained; this renders any discussion of the mechanism by which clusters are formed meaningless. If any of these compounds show unusual behavior, synthetic strategies can be improved at a later date.

Reactions of various hydrated cobalt(II) salts with 2 equiv of Hchp, $^1/_6$ equiv of RPO_3H_2, and 2 $^1/_3$ equiv of NEt_3 in MeCN give a deep-purple solution. This was evaporated to dryness and extracted with CH_2Cl_2; deep-purple crystals could be grown by layering with hexane. The observations made during reaction are identical for a range of phosphonates; however, the structures of the crystalline materials obtained are not the same in all cases.

The most common stoichiometry observed, $[Co_{14}(OH)_2(X)_2(chp)_{20}(O_3PR)_2(H_2O)_2]$ (where X = OH for perchlorate and X = F for tetrafluroborate as starting materials), was found for five different phosphonates—R = CH_2Ph **1**, Me **2**, Et **3**, *n*-octyl **4**, and H **5** (**1** and **3** contained X = OH whereas **2**, **4**, and **5** contained X = F). In the case of **5**, a further two terminal Hchp ligands are attached to the core. The structures of these tetradecanuclear complexes are all similar (Figure 1), differing only in the alkyl group on the phosphonate. In each case, the cluster lies about an inversion center (Figure 1). The seven Co centers in the asymmetric unit lie in a plane, with four of the centers (Co(3), Co(5), Co(6), and Co(7)) surrounding a fifth [Co(4)], bridged through μ_3-OH atoms in an array similar to the repeating pattern found in cobalt hydroxide, and also found at the core of large clusters, e.g., $\{Fe_{19}\}$ cages.[22] The other two cobalt sites in the asymmetric unit (Co(1) and Co(2)) are attached to this pentametallic fragment through the phosphonates. The phosphonates also bridge to the second half of the molecule,

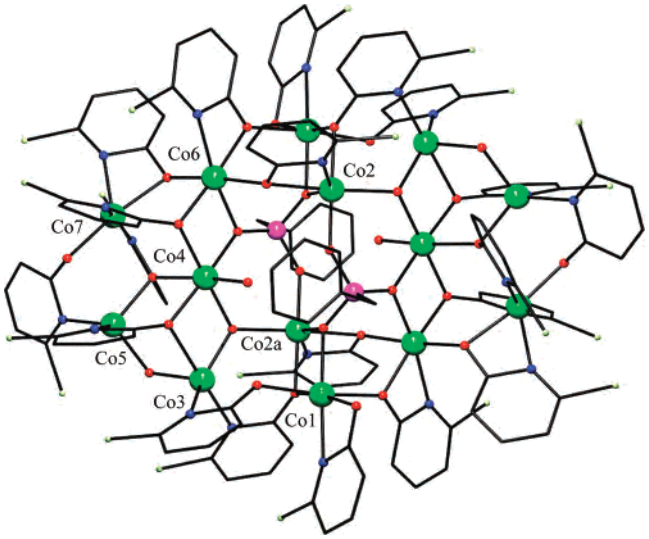

Figure 1. Structure of **1** in the crystal. Color scheme: Co, green; P, magenta; N, blue; O, red; C, black lines; Cl, light green.

which is symmetry equivalent to the first half. The structure has a distinct "step", perhaps best quantified by considering the angle between the mean plane of the Co centers in the asymmetric unit and the central Co(1), Co(2), Co(1a), and Co(2a) section, which is 56.4°. The two phosphonates therefore disrupt the regular "$Co(OH)_2$" structure and link together two planes.

Six of the cobalt sites are six-coordinate, and the seventh (Co(5)) is four-coordinate; the coordination sites do not have regular geometries, as is common for cobalt(II). One of the oxygen atoms of each phosphonate bridges two cobalt sites (Co(4) and Co(6)) while the second binds only to Co(2). The third O atom bridges to the symmetry equivalent fragment, bridging Co(2a) and Co(1a). The phosphonate therefore shows the 5.221 bridging mode (Harris notation;[23] see Scheme 1). The chp ligands coat the exterior of the cluster, and as typical, show a variety of coordination modes. Of the 10 chp ligands in the asymmetric unit, 7 show the 2.21-mode, 2 the 2.11 mode, and 1 the chelating 1.11 mode.

While five different phosphonates give this tetradecanuclear structure, other phosphonates lead to other cages. When fluorophosphonic acid is used with hydrated cobalt tetrafluoroborate, an undecanuclear cage **6** resulted: the structure (see below) led to an examination of phosphoric acid itself, which gives an isostructural and possibly identical compound **7**. Reaction with pyrophosphonic acid also led to the same compound. The formula is $[Co_{11}(E)(chp)_{18}(PO_4)]$, with E = either fluoride or hydroxide; elemental analysis of **6** supports the presence of a fluoride, presumably derived from either tetrafluoroborate or fluorophosphonate. In the synthesis of **6**, it is assumed that the phosphate is derived from hydrolysis of fluorophosphonate.

(20) Midollini, S.; Orlandini, A.; Rosa, P.; Sorace, L. *Inorg. Chem*. **2005**, *44*, 2060−2066.
(21) Langley, S.; Helliwell, M.; Raftery, J.; Tolis, E. I.; Winpenny, R. E. P. *Chem. Commun*. **2004**, 142−143.
(22) Goodwin, J. C.; Sessoli, R.; Gatteschi, D.; Wernsdorfer, W.; Powell, A. K.; Heath, S. L. *J. Chem. Soc., Dalton Trans.* **2000**, 1835−1840.
(23) Harris notation describes the binding mode as $[XY_1Y_2Y_3...Y_n]$, where *X* is the overall number of metals bound by the whole ligand and each value of *Y* refers to the number of metal atoms attached to the different donor atoms. See: Coxall, R. A.; Harris, S. G.; Henderson, D. K.; Parsons, S.; Tasker, P. A.; Winpenny, R. E. P. *J. Chem. Soc., Dalton Trans.* **2000**, 2349−2356.

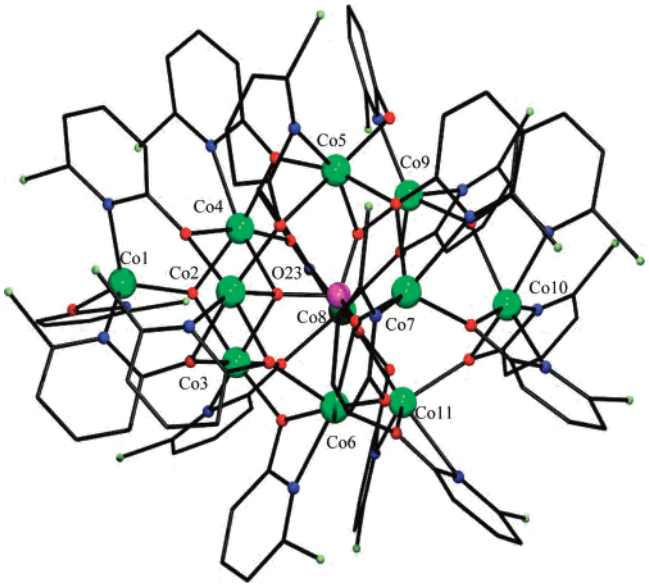

Figure 2. Structure of **6** in the crystal. Color scheme as in Figure 1.

Scheme 1. Observed Bonding Modes of Phosphonate and Pyridonate Ligands

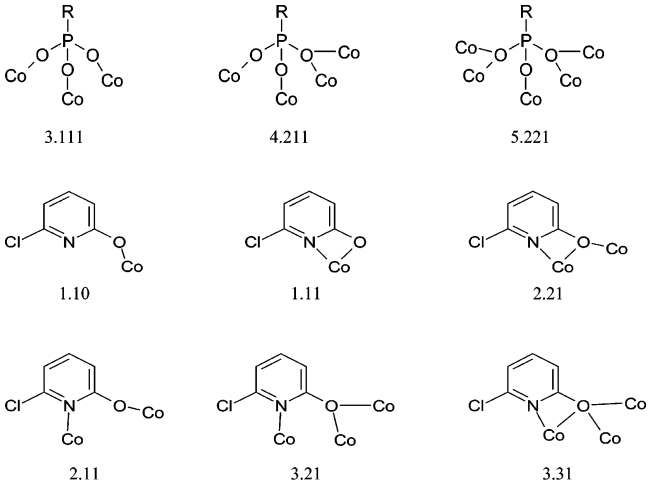

The structure (Figure 2) has approximately three-fold symmetry. It contains a central phosphate, showing a 9.3222 binding mode; the nine Co centers bound to the phosphate form a triangle (Co(2), Co(3), Co(4)) bound to the μ_3-O atom of the phosphate above six Co centers (Co(5)−Co(9), Co(11)) with a "chair" conformation. This array could be considered an icosahedron missing one triangular face. The 10th and 11th Co centers cap the triangle (Co(1)) and chair (Co(10)). The structure can be described in four sections, beginning at Co(1), which we will consider the "top" of the cluster. This center is four-coordinate, bound to a μ_3-hydroxide/fluoride (O(23)), the O atom of a 1.10-bound chp, and two N atoms of two 3.21-bound pyridonates. The O atoms of the 3.21-bound pyridonates and the μ_3-OH bridge the edges of the next section, the triangle consisting of Co(2), Co(3), and Co(4). Bridging all three metals and beneath the triangle is the μ_3-O atom from the phosphonate. There is a single chelating 2.21-pyridonate attached to each of these metals, and the O atom of these bridges to the "chair" of cobalt centers below. The final coordination site on each of the Co(2), Co(3), and Co(4) atoms is occupied by a O atom from a further 2.21-chp ligand, with these chp ligands chelating to Co sites within the chair.

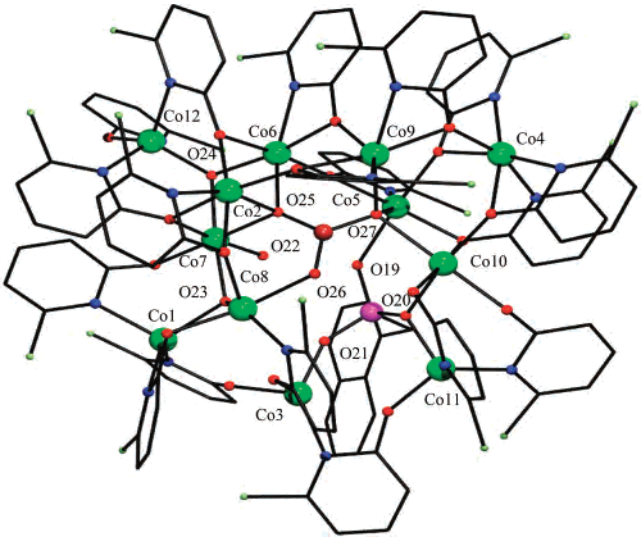

Figure 3. Structure of **8** in the crystal. Color scheme as in Figure 1.

The six Co sites in the chair are bound to the μ_2-O atoms of the 9.3222 phosphonate. Three of them (Co(5), Co(6), and Co(8)) are six-coordinate, and the others (Co(7), Co(9), and Co(11)) are five-coordinate. The former three sites are bound to chp ligands that chelate and bridge between the centers within the chair and the triangle, while the latter sites also bind to an O atom from a 2.21 ligand which chelates to the final metal in the structure, Co(10). This metal is bound to three 2.21-pyridonates, with a fac geometry; this creates a $[Co(chp)_3]^-$ "complex ligand" and it is these three O atoms that bind to Co(7), Co(9), and Co(11) of the chair. This $[Co(chp)_3]^-$ fragment has been seen previously as part of cluster structures.[3] The 18 chp ligands exhibit four modes of bonding: 12 are 2.21, 3 are 2.11, and 2 are 2.21, with a single terminal chp in the 1.10 mode.

When R is a napthylmethyl group using hydrated cobalt tetrafluoroborate as the starting salt, we can make a dodecanuclear cage: $[Co_{12}(OH)_2(chp)_{18}(O_3PCH_2Nap)(BO_3H)(H_2O)]$ (**8**) (Figure 3). This has a very irregular structure and presents the problem of assigning a 7.331 bridging tetraatomic fragment found at the center of the structure. It is a planar triangle; however, assignment as nitrate or carbonate does not account for the bond lengths of ca. 1.42 Å. The best explanation appears to be BO_3H^{2-}. The two μ_3-atoms (O(25) and O(27)) are assigned as O, while the atom bound to a single metal (O(26)) is that of the B−OH. Supporting evidence comes from charge balance, which is straightforward if BO_3H^{2-} is present, and a O···O contact of 2.66 Å between the OH group and an O atom from a chp ligand; such a short contact indicates the presence of a proton between the O atoms, and the chp is deprotonated.

The overall structure is heavily dependent on this central group. Two $\{Co_4\}$ fragments are attached to the μ_3-O atoms of the BO_3H; both are heavily distorted and incomplete heterocubanes (Co(2), Co(6), Co(7), and Co(12) and Co(4), Co(5), Co(9), and Co(10)). These distorted heterocubanes

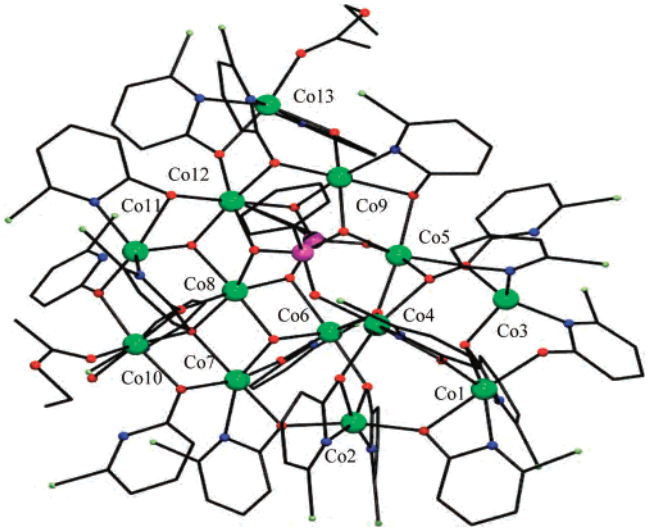

Figure 4. Structure of **9** in the crystal. Color scheme as in Figure 1.

are linked through the hydrogenborate and through O atoms from pyridonates.

The OH of the BO_3H binds to Co(8), which is bridged to Co(1) and Co(3); on the other side of the cluster, the phosphonate occupies a similar position to Co(8), bridging to Co(11) and Co(3). The phosphonate has the 4.211 binding mode in this structure. The 18 chp ligands show four modes: 9 show the 2.21 mode, 5 the 2.11 mode, 3 the 3.21 mode, and 1 the terminal 1.10 mode. There are two four-coordinate cobalt sites (Co(3) and Co(12)) and two five-coordinate cobalt sites (Co(1) and Co(11)), with the remainder six-coordinate. In all cases, the coordination geometries are distorted.

Reactions of hydrated cobalt tetrafluoroborate and perchlorate with phenylphosphonic acid led us to isolate the known $[Co_{13}(OH)_3(chp)_{19}(O_3PPh)_2(H_2O)_2(EtOAc)_2]$ (**9**) cage (Figure 4).[24] The synthetic method given here is different from the published procedure. Comparing **9** to **1**−**5**, one can see structural similarites most clear around Co(8); as in **1**, five other cobalt sites (Co(6), Co(7), Co(10), Co(11), and Co(12)) are attached to this site through μ_3-O atoms creating a planar array similar to that of cobalt hydroxide, with the sixth site taken up by the phosphorus atom. The remaining cobalt sites lie in irregular positions.

While cobalt tetrafluoroborate and perchlorate show identical reactivity with phenylphosphonic acid, reaction with hydrated cobalt nitrate gives a different product—presumably due to the coordinating ability of the anion. (A complication in understanding the chemistry in this system arises because it is not always possible to crystallize clusters with differing anions with the same phosphonate ligands.)

With phenylphosphonate and hydrated cobalt nitrate, an octanuclear compound $[HNEt_3][Co_8(chp)_{10}(Hchp)_2(O_3PPh)_2(NO_3)_3]$ (**10**) results (Figure 5), previously communicated.[17] Here the two P atoms P(1) and P(2) from phosphonate and four Co atoms Co(3), Co(4), Co(5), and Co(6) lie on the vertices of a trigonal prism. The final four Co atoms Co(1), Co(2), Co(7), and Co(8) lie above the triangular faces of the prism. The phosphonates both show the 4.211 mode, while eight of the chp ligands bind with the 2.21 mode, two with the 3.21 mode, and two exhibit the terminal 1.10 mode. Two of the Co(II) ions are five-coordinate (Co(4) and Co(6)) while the remainder are six-coordinate with distorted geometries. The structure also contains two chelating nitrates binding to Co(1) and Co(8), respectively, and a 2.11 bridging nitrate, bridging Co(3) and Co(5).

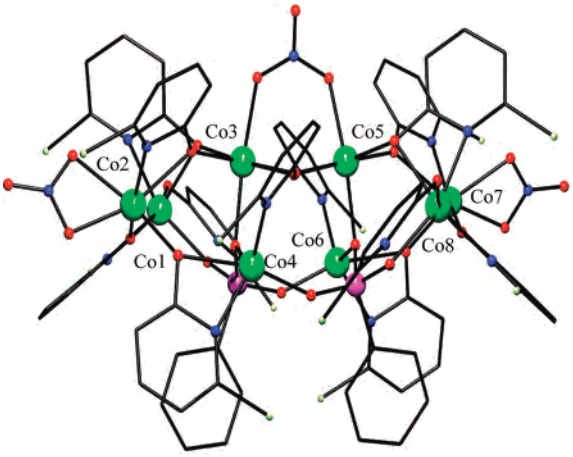

Figure 5. Structure of **10** in the crystal. Color scheme as in Figure 1.

Complex **10** is an anion, and a NEt_3H cation is found in the crystal lattice. This forms a significant H bond to the chelating nitrate groups from neighboring $\{Co_8\}$ clusters, leading to a one-dimensional (1D) chain forming in the crystal. This intermolecular interaction may be important in understanding the magnetic behavior of this molecule.

In studies of cobalt−pivalate cages, it was found[25] that the nuclearity of the compounds formed could be influenced by the addition of hydrogen peroxide. When a few drops of hydrogen peroxide solution were added to the reaction mixture that gives **10**, the solution turns dark brown. The crystals that result from this procedure contain a centrosymmetric icosanuclear cluster $[Co_{20}(O)_2(OH)_4(chp)_{26}(PhPO_3)_4(H_2O)_6]$ (**11**) (Figure 6), with a structure related to the tetradecanuclear clusters **1**−**5** and **9**. The resemblance is most clear around Co(4); as in **1**, for example, four other cobalt sites (Co(1), Co(2), Co(3), and Co(8)) are attached to this site through μ_3-O atoms, creating a planar array similar to that of cobalt hydroxide.

The phosphonates are attached to the edge of this fragment, bridging to further cobalt sites (Co(5) and Co(6)); these three sites are out of the plane described by Co(1)−Co(4) and Co(8). This is similar to the role Co(1) and Co(2) play in the structure of **1**. The big difference arises in the center of the cluster, where Co(9) and Co(10) and their symmetry equivalents are found. If Co(7) and its symmetry equivalent were included, this fragment would form a distorted face-sharing dicubane fragment, which would link the two planar cobalt hydroxide units. The structure is mixed-valent, with

(24) Brechin, E. K.; Coxall, R. A.; Parkin, A.; Parsons, S.; Tasker, P. A.; Winpenny, R. E. P. *Angew. Chem., Int. Ed.* **2001**, *40*, 2700−2703.

(25) Aromi, G.; Batsanov, A. S.; Christian, P.; Helliwell, M.; Parkin, A.; Parsons, S.; Smith, A.; Timco, G. A.; Winpenny, R. E. P. *Chem.—Eur. J.* **2003**, *9*, 5142−5161.

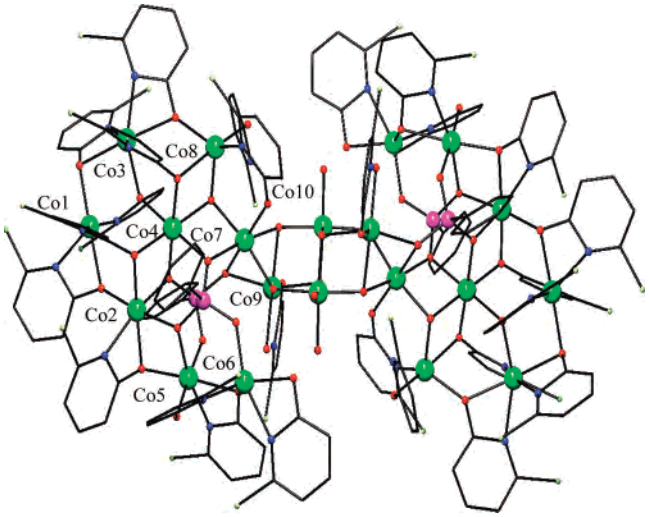

Figure 6. Structure of **11** in the crystal. Color scheme as in Figure 1.

18 cobalt(II) sites and 2 cobalt(III) sites. The cobalt(III) ions are Co(10) and its symmetry equivalent; this is clear from bond lengths (1.88−1.95 Å) and the regular coordination geometry (trans angles 173.0−175.5°, cis angles 83.0−94.5°) of this site. The two atoms bridging within the shared face of the bicubane are μ_3-oxides; if the unit were regular these would be μ_4-oxides, but the final contact (to Co(7)) is 3.25 Å. Both the bridging oxide and the Co(III) centers arise from the use of peroxide; previously, it has been shown that peroxide can partially oxidize cobalt in a range of mixed-valent cobalt−pivalate cage complexes.[25]

Of the nine cobalt(II) sites in the asymmetric unit, two are five-coordinate (Co(6) and Co(8)), while the remaining seven are six-coordinate. Both phosphonate ligands show the 5.221 binding mode. The 13 unique chp ligands show 6 bonding modes: 5 bind as 2.21, 2 as 3.31, 2 as 3.21, 2 as 2.11, 2 as 1.10, and 1 as 1.11. There are also four μ_3-bridging hydroxides and six terminal water molecules in the structure; all these single O atom ligands are found associated with the central region of the molecule around Co(9), Co(10), and their symmetry equivalents. An intricate series of H bonds are present between these atoms and also the O and N atoms of chp ligands.

With *tert*-butylphosphonate and hydrated cobalt nitrate, a hexanuclear compound results: $[Co_6(chp)_8(O_3P^tBu)_2(Hchp)_2(H_2O)_2]$ (**12**) (Figure 7). This contains a centrosymmetric plane of six cobalt centers; within the asymmetric unit the three cobalt sites are bridged by a 3.111 phosphonate. The two halves of the molecule are held together by two μ_2-oxygens from a 2.21 chp ligand. The asymmetric unit contains three 2.21 chp ligands, one 2.11 and one terminal 1.10 pyridonate. Terminal water molecules are found attached to Co(3) and its symmetry equivalent and form two H bonds to oxygen atoms from chp and O_3P^tBu groups. Co(3) is six-coordinate and Co(1) and Co(2) are five-coordinate. Compared with the complexity of the other clusters, this cage seems quite restrained.

Given the success of these simple reactions, the chemistry has been extended a little further. If ethylenediphosphonic acid is reacted with hydrated cobalt tetrafluoroborate in a

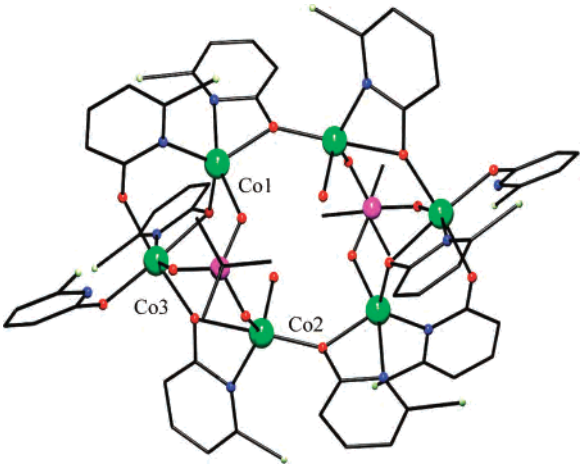

Figure 7. Structure of **12** in the crystal. Color scheme as in Figure 1.

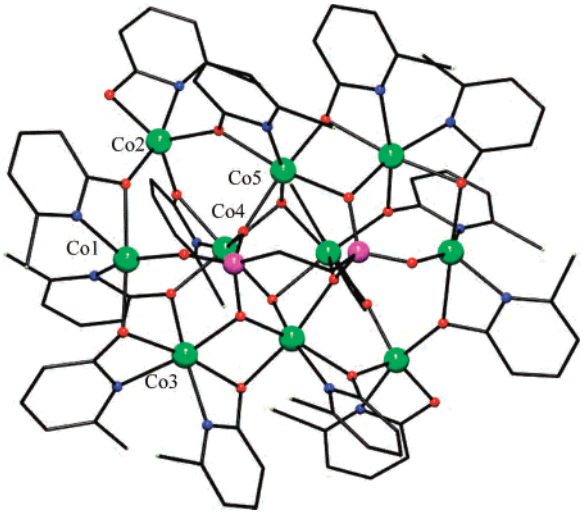

Figure 8. Structure of **13** in the crystal. Color scheme as Figure 1.

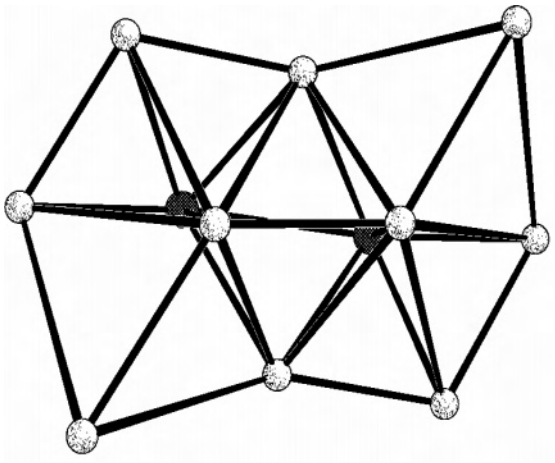

Figure 9. Hexacapped octahedral core of **13**.

similar manner, a decanuclear cage $[Co_{10}(OH)_2(chp)_{14}(O_3PCH_2CH_2PO_3)]$ (**13**) (Figure 8) can be made. Complex **13** lies disposed about a crystallographic two-fold axis.

The 10 Co and 2 P sites of the molecule lie on the vertices of an octahedron that is capped on 4 faces and 2 edges, giving an elongated hexagonal bipyramid (Figure 9). Co(4), Co(5), and their symmetry equivalents and the two P sites form the octahedron. Both PO_3 end groups of the diphosphonate show

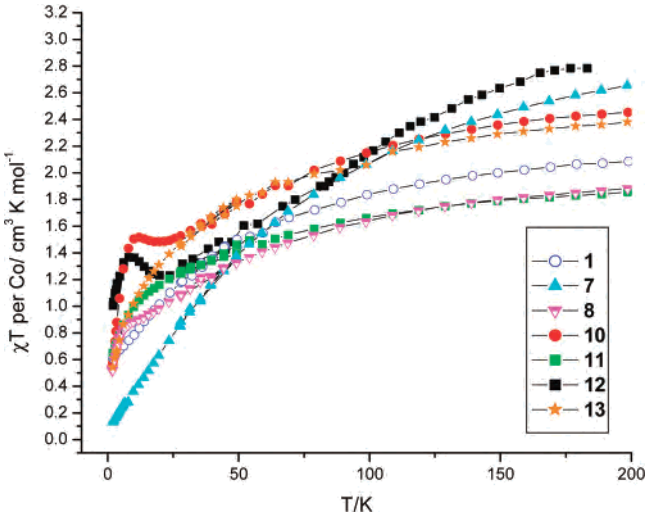

Figure 10. Variation of $\chi_m T$ per cobalt with T measured at 1000 G.

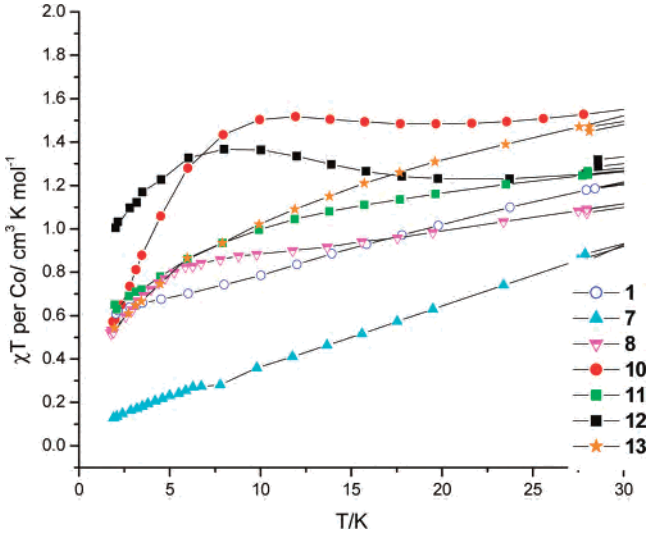

Figure 11. Variation of $\chi_m T$ per cobalt with T measured at 1000 G.

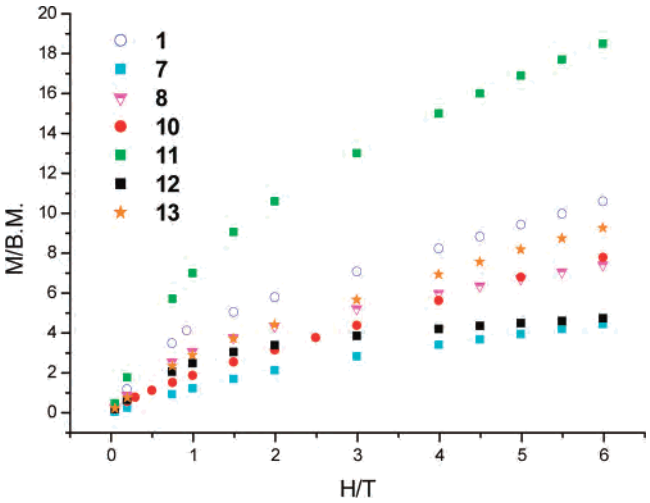

Figure 12. Variation of magnetization (M) with field, measured at 1.8 K.

a 5.221 binding mode, but two Co sites (Co(5) and its symmetry match) are bound to both PO_3 groups. The overall binding mode of the diphosphonate is therefore 8.221221.

As in all these structures, the binding mode of the chp ligands is variable. Of the seven unique chp groups, five show the 2.21 mode, one the 3.21 mode, and one the chelating 1.11 mode. There are also two μ_3-hydroxides in the structure. Two of the Co sites in the asymmetric unit are five-coordinate (Co(1) and Co(2)), and the remaining three sites are six-coordinate.

Magnetic Measurements. The synthetic and structural studies give seven new crystalline cobalt clusters. The variable-temperature magnetic behavior of **1**, **7**, **8**, and **10**−**13**, represented as $\chi_m T$ against T (where χ_m is the molar magnetic susceptibility), is shown in Figure 10. To make comparison between the different clusters easier, the data is plotted *per cobalt center*. The data per formula unit is given in Supporting Information.

Explanation of the magnetic behavior of cobalt(II) complexes is always difficult, due to the orbitally degenerate ground state of the ion when six-coordinate. For this reason, derivation of the magnitude of the exchange interactions between cobalt centers is impossible, especially in cases such as those here where the structures are extremely complicated.

The high-temperature value of $\chi_m T$ per cobalt varies between the seven clusters. Making the assumption that exchange interactions are of similar magnitude in each case, the high-temperature value should be dependent on the sum of the single ion contributions. In turn, this should be dependent on the g values of the individual cobalt(II) centers. The g value for mononuclear Co(II) complexes is dependent on geometry, so we examined whether this high-temperature value depended on the percentage of six-coordinate sites in the cluster. There is a weak correlation; the highest value of $\chi_m T$ per Co is found for **12**, where only one-third of the sites are six-coordinate. Complexes **1**, **7**, **10**, **12**, and **13** follow an approximately linear trend, with the smallest high-temperature value of $\chi_m T$ found for **1** and **13**, which have 86 and 80% of six-coordinate Co sites, respectively. Complexes **8** and **11** do not fit the trend; **11** is mixed-valent, which may account for the anomalously low value, but there is no simple explanation for the case of **8**. This trend—such as it is—may be coincidental.

All seven compounds show a steady decrease in $\chi_m T$ as T falls. This is largely due to single ion effects of Co(II), and deriving any information about exchange contributions to the temperature-dependent behavior is impossible. However, below about 30 K, the behavior of the clusters diverges considerably (Figure 11).

For four of the clusters, **1**, **7**, **11**, and **13**, the value of $\chi_m T$ continues to fall, although only for **7** is the value approaching zero at the lowest temperature measured. For **8** there is a distinct plateau from around 18 to 5 K, below which the value of $\chi_m T$ begins to fall again. For **10** and **12**, there are maxima in $\chi_m T$ at ca. 8 and 10 K, respectively. It seems reasonable to assume that the plateau in **8** and maxima in **10** and **12** reflect nondiamagnetic ground states for these clusters. Magnetization studies do not help; no saturation is seen for any of the compounds up to 6 T external field at 1.8 K (Figure 12). Given the high anisotropy of the ions present and the high nuclearity of the clusters, this is unsurprising.

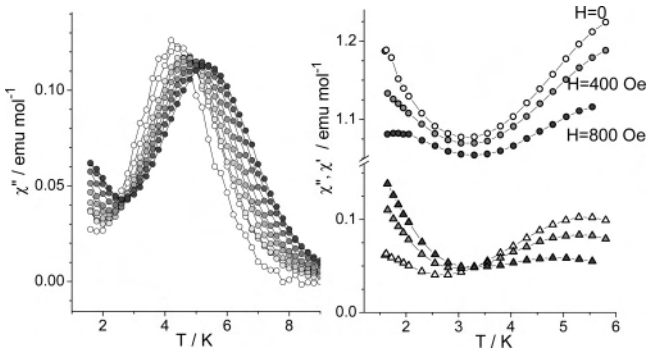

Figure 13. (left) Frequency-dependent behavior of χ'' for **10** in zero static field for nine logarithmically spaced frequencies between 160 and 20 000 Hz. (right) Temperature dependence of χ' (circles) and χ'' (triangles) measured at 19 010 Hz in different applied static fields.

Measurements of ac susceptibility were previously performed[17] on **10** and revealed frequency-dependent maxima in χ'' against T, where χ'' is the out-of-phase susceptibility, and a second rise in χ'' at lower temperature. Therefore, compounds **8** and **12** were investigated, as they show an increase of the χT product below 20 K. In neither case was an out-of-phase signal detected above 1.8 K. In this series of compounds, **10** appears to be unique in showing slow relaxation of magnetization. Analysis of the ac data for **10** using an Arrhenius law ($\tau = \tau_0 \exp(\Delta/k_B T)$, where τ is the relaxation time derived from the ac measurement), it was found that different samples gave different energy barriers and a range of pre-exponential factors: one sample gave $\Delta = 84(\pm 2)$ K and $\tau_0 = 1.8(\pm 3) \times 10^{-12}$ s; a second gave $\Delta = 80(\pm 2)$ K and $\tau_0 = 2.1(\pm 3) \times 10^{-11}$ s. Therefore, while the energy barrier is moderately consistent and very high for a single-molecule magnet (SMM), the pre-exponential factor varies by an order of magnitude between samples. There are three previous examples of Co(II) cages showing behavior similar to that of SMMs.[26]

A possible explanation of the peculiar behavior of **10** could come from its 1D network of H bonds. To confirm this hypothesis, the ac susceptibility was measured under field, and we discuss here in detail results which were only mentioned in the previous communication.[17] In Figure 13, the value of χ'' measured in zero applied field for frequencies ranging between 160 and 20 000 Hz is reported, together with the field dependence for a selected frequency, 19 010 Hz. Two peaks in χ'' are observed, but the application of a static field shows a different behavior for the peak observed around 5 K, compared with the one that appears at lower temperature. A marked increase of χ'' is observed for the lower temperature peak on application of a static field. This last behavior is generally observed in SMMs, when the application of a field hampers or reduces the tunneling by removing the energy degeneracy of pairs of states.[7,10] The relaxation rate decreases, and the peaks in χ'' shift to higher frequency. On the other hand, the application of an external static field *decreases* the amplitude of the higher temperature χ'' peak and slightly shifts the maximum to lower temperatures. Also, the real component χ' is significantly depressed by the application of a static field.

These data suggest that a moderate field has a stronger influence on the equilibrium susceptibility associated with this "5 K" peak rather than on the dynamic of the magnetization. This is typical of systems showing a short-range correlation of the magnetic moments, for example, in 1D magnetic structures.[27]

In **10**, the 1D magnetic structure could be due to the H-bond network, and the high-temperature peak in χ'' could thus reflect the contributions to the energy barrier coming from both the isolated cluster anisotropy and intercluster interactions[28] and the simultaneous suppression of tunneling. In fact, the intrachain exchange interaction acts as an internal bias field that removes the energy degeneracy also in the zero external field.[29] The application of a moderate external field is therefore expected to have minor effects on the dynamics of SMMs arranged in a 1D structure, as indeed observed for **10**. However, due to the presence of disorder in the solvent of crystallization, segments of different lengths are expected. These are characterized by different timescales for the relaxation, as the relaxation is expected to depend linearly on the length of the segments.[30] It has been shown that the average length of the segments affects the pre-exponential factor in the Arrhenius law, without altering the energy barrier.[30] The differences observed in the two investigated samples of **10** could then be ascribed to a different content of disordered solvent and thus to a different average length of the segments. Very short segments or oligomeric species can instead relax through a collective reversal of all the spins of the segment and therefore behave like SMMs,[31] showing quantum tunneling features such as the strong effect of the static field on the χ'' value. The low-temperature peak can be tentatively assigned to very short segments of interacting clusters, but in this case, the relaxation time is expected to scale exponentially with the length. This justifies the very large distribution of the relaxation times observed and thus the small value of χ'' compared with that of χ'.

In **8** and **12**, no H-bonding network is present and fast relaxation prevents the observation of a nonzero χ''. Therefore, it is probably best to regard **10** as an unusual SCM

(26) (a) Yang, E.- C.; Hendrickson, D. N.; Wernsdorfer, W.; Nakano, M.; Zakharov, L. N.; Sommer, R. D.; Rheingold, A. L.; Ledezma-Gairaud, M.; Christou, G. *J. Appl. Phys.* **2002**, *91*, 7382−7384. (b) Murrie, M.; Teat, S. J.; Stöeckli-Evans, H.; Güdel, H. U. *Angew. Chem., Int. Ed.* **2003**, *42*, 4653−4656. (c) Zeng, M.-H.; Yao, M.-X.; Liang, H.; Zhang, W.-X.; Chen, X.-Mi. *Angew. Chem., Int. Ed*. **2007**, *46*, 1832−1835.

(27) Steiner, M.; Villain, J.; Windsor, C. G. *Adv. Phys.* **1976**, *25*, 87−209.

(28) (a) Clérac, R.; Miyasaka, H.; Yamashita, M.; Coulon, C. *J. Am. Chem. Soc*. **2002**, *124*, 12837−12844. (b) Coulon, C.; Clérac, R.; Lecren, L.; Wernsdorfer, W.; Miyasaka, H. *Phys. Rev. B: Condens. Matter Mater. Phys.* **2004**, *69*, 132408. (c) Ferbinteanu, M.; Miyasaka, H.; Wernsdorfer, W.; Nakata, K.; Sugiura, K.; Yamashita, M.; Coulon, C.; Clérac, R. *J. Am. Chem. Soc.* **2005**, *127*, 3090−3099. (d) Coulon, C; Miyasaka, H.; Clérac, R. *Struct. Bond*. **2006**, *122*, 163−206

(29) Wernsdorfer, W.; Allaga-Alcalde, N.; Hendrickson, D. N.; Christou, G. *Nature* **2002**, *416*, 406−409.

(30) Bogani, L.; Caneschi, A.; Fedi, M.; Gatteschi, D.; Massi, M.; Novak, M. A.; Pini, M. G.; Rettori, A.; Sessoli, R.; Vindigni, A. *Phys. Rev. Lett.* **2004**, *92*, 207204/1−207204/4.

(31) Vindigni, A.; Rettori, A.; Bogani, L.; Caneschi, A.; Gatteschi, D.; Sessoli, R.; Novak, M. A. *Appl. Phys. Lett.* **2005**, *87*, 073102/1−073102/3.

rather than as a SMM. Both the energy barrier and the pre-exponential factor are similar to those observed previously for SCMs,[32] e.g., $\Delta/k_B = 154$ K, $\tau_o = 3.0(2) \times 10^{-11}$ s for $[Co(hfac)_2(NITPhOMe)]_n$.[33]

Discussion and Conclusions

There is huge scope when it comes to using phosphonates in polynuclear chemistry. From minor variations in reaction procedure, seven new structural types can be made, varying in nuclearity from a $\{Co_6\}$ cage to a $\{Co_{20}\}$ cage. While the growth in polymetallic chemistry has been considerable, these compounds are still among the largest cobalt(II) cages reported.[1]

Unlike some recent cluster chemistry, for example, the reports of Mn rods based on linked triangles by Brechin and co-workers,[34] there is no unifying structural theme to the cages discussed here. There are, however, two themes. Several of the clusters, **1**−**5**, **9**, and **11**, can be related to cobalt hydroxide. A similar structure was reported previously which contained 24 cobalt(II) ions.[35] Although the structures contain fragments which contain μ_3-bridging hydroxides leading to sections which are planar, e.g., in **1**−**5** and **11** there are $\{Co_6\}$ units which are almost flat, the overall structures all contain a "step". In **1**−**5** and **9**, the step occurs where the phosphonate ligands bind to the cage, while in **11** the discontinuity is due to the Co(III) cubane. Again, the phosphonate binds to the edge of the planar section of the cage. It is possible that in these discrete clusters the phosphonates are distorting the structures away from planarity. This is possibly because of the large number of metal sites bound to each RPO_3^{2-} ligand, for example, the 5.221 binding mode is not compatible with the regular flat structure of cobalt hydroxide. Where cobalt phosphonates are found in 2D arrays, the bonding modes seen are normally the 4.221 or 3.111 modes.[16,36] The 4.221 mode forms layers via edge-sharing CoO_6 octahedra, usually with a terminal water molecule making up the sixth coordination sphere. The phosphonates cap the layers alternately above and below the plane of the layer. The 3.111 mode forms planar "staircase" chains again, with the phosphonates alternately above and below the plane of the layer.[16,36] Compound **12** also contains a planar array, albeit a much smaller hexanuclear array and without bridging hydroxides, and contains the only 3.111 phosphonate found in this study. This shows an arrangement of metals and phosphonates similar to that found in the 2D array; however, the chp ligands present in **12** cap the outside of the cage, halting any further growth. Very speculatively, **12** might be considered an early stage of growth of the larger structures.

Table 2. Bond Length Ranges (Å) by Bonding Mode and Coordination Number[a]

	four-coordinate Co(II)	five-coordinate Co(II)	six-coordinate Co(II)
		chp	
1.**1**0[b]	1.923−1.935	2.000	2.003−2.130
1.**1**1		2.050	2.066−2.099
1.1**1**		2.230	2.181−2.256
2.**1**1	1.960	2.037	1.975−2.132
2.1**1**	2.038−2.085	2.047−2.083	
2.20		2.200	2.030−2.091
2.**2**1	1.964−1.971	1.969−2.324	1.982−2.347
2.2**1**		2.059−2.445	2.041−2.297
3.**2**1		2.239	2.036−2.305
3.2**1**	2.021−2.071	2.066−2.118	2.073−2.158
3.30			2.170−2.236
3.**3**1	2.029−2.082		2.045−2.399
3.3**1**			2.120−2.231
		RPO_3^{2-}	
3.111		1.938−1.984	2.108
4.**2**11	1.987	2.033−2.036	2.113−2.123
4.2**1**1	1.946	1.939−1.940	2.035−2.081
5.**2**21[c]			2.011−2.235
5.22**1**[c]		1.987−2.020	1.982−2.083
9.**3**222			2.119−2.154
9.3**2**22		2.018−2.040	2.064−2.084

[a] E.s.d's in the range of (2)−(18). [b] Harris notation follows Cahn−Ingold−Prelog priority rules; therefore, for chp the second number refers to the number of metal centers bound to the O atom and the third number refers to the number bound to the N atom. [c] Includes bond lengths involving the 8.221221 diphosphonate in **13**.

The second theme concerns the structures which contain a small oxygen donor anion at the center of the cage. In **6** and **7**, the anion is phosphate, derived in one instance from hydrolysis of FPO_3H_2; in **8**, the anion is $[BO_2(OH)]^{2-}$, derived from hydrolysis of tetrafluoroborate. In **6** and **7**, the 9.3222 mode of the PO_4^{3-} ion creates a structure where a Co(II) triangle is attached to a $\{Co_6\}$ chair; if the triangle were repeated on the other side of the chair an icosahedron would result (and the bonding mode of the phosphate would be 12.3333); however, the regularity is broken. The presence of this central anion seems to have a strong structure-directing role in **6**−**8**. In **10**, nitrate is found bound to the cluster, but on the exterior rather than at the center.

The observation of the cobalt hydroxide fragments in some structures and the strong influence of the central anion in others suggest that the phosphate−pyridonate reaction matrix has little structure-directing potential in itself; deliberate addition of templates to this reaction matrix could therefore lead to "control" of structures in the future.

The various phosphonates used lead to different structures. Phenylphosphonate produces a range of structures (**9**−**11**) which we cannot make with alkylphosphonates. Alkylphosphonates seem to favor the planar $\{Co_{14}\}$ structure (**1**−**5**). Naphthylphosphonate and *t*-butylphosphonate give unique structures (**8** and **12**, respectively); whether this is because these ligands are sterically demanding remains unproven.

Bond length ranges for the various ligands, coordination modes, and coordination numbers show predictable variations

(32) Coulon, C.; Miyasaka, H.; Clérac, R. *Struct. Bonding* **2006**, *122*, 163−206.
(33) Caneschi, A.; Gatteschi, D.; Lalioti, N.; Sangregorio, C.; Sessoli, R.; Venturi, G.; Vindigni, A.; Rettori, A.; Pini, M. G.; Novak, M. A. *Angew. Chem., Int. Ed.* **2001**, *40*, 1760−1763.
(34) Rajaraman, G.; Murugesu, M.; Carolina Sañudo, E.; Soler, M.; Wernsdorfer, W.; Helliwell, M.; Muryn, C.; Raftery, J.; Teat, S. J.; Christou, G.; Brechin, E. K. *J. Am. Chem. Soc*. **2004**, *126*, 15445−15457.
(35) Brechin, E. K.; Harris, S. G.; Harrison, A.; Parsons, S.; Whittaker, G. A.; Winpenny, R. E. P. *Chem. Commun*. **1997**, 653−654.
(36) (a) Cao, D. K.; Gao S.; Zheng, L.-M. *J. Solid State Chem.* **2004**, *177*, 2311−2315. (b) Bauer, E.; Bellitto, C.; Colapietro, M.; Ibrahim, S.; Mahmoud, M.; Portalone, G.; Righini, G. *J. Solid. State Chem*. **2006**, *179*, 389−397. (c) Yi, X.; Zheng, L.-M.; Xu, W.; Chen, J.-S. *Dalton Trans.* **2003**, 953−956.

(Table 2). Thus, for a given coordination mode of the ligand, the bond length, on average, increases with the coordination number of the cobalt. Similarly, for a given coordination number of Co(II), the O−Co bond length increases with the number of metal centers attached to the oxygen donor atom. In most cases there is some overlap of the bond length ranges.

The magnetic properties of the cages are intriguing, and difficult to explain. Compound **10** shows slow relaxation of magnetization and other cages appear to have nondiamagnetic ground states (**8** and **12**). Magnetic studies of Co(II) cages are notoriously difficult. A recent paper by Cotton, Tsukerblat, and co-workers illustrates the problem:[37] Modeling the magnetic behavior of an equilateral Co(II) triangle can be achieved, but requires four parameters ($g_{\|}$, $g_{\perp}$, J, and G, where G is the anisotropic exchange and the other symbols have their usual meanings). For a $Co(II)_4$ heterocubane, these authors can model the data down to 10 K, but below that point, it becomes impossible due to significant orbital effects. Strategies have been devised to deal with cobalt(II) ions, but generally in low-nuclearity complexes.[38] Here, the high nuclearity and low symmetry makes it impossible to conceive of a way of modeling the variable-temperature magnetic data.

(37) Berry, J. F.; Cotton, F. A.; Liu, C. Y.; Lu, T.; Murillo, C. A.; Tsukerblat, B. S.; Villagran, D.; Wang, X. *J. Am. Chem. Soc.* **2005**, *127*, 4895−4902.

(38) (a) Lines, T. *Phys. Rev.* **1963**, 546−555. (b) Clemente-Juan, J. M.; Coronado, E.; Gaita-Arino, A.; Gimenez-Saiz, C.; Güdel, H.-U.; Sieber, A.; Bircher, R.; Mutka, H. *Inorg. Chem.* **2005**, *44*, 3389−3395. (c) Sakiyama, H.; Ito, R.; Kumagai, H.; Inoue, K.; Sakamoto, M.; Nishida, Y.; Yamasaki, M. *Eur. J. Inorg. Chem.* **2001**, 2027−2032. (d) Sakiyama, H. *Inorg. Chim. Acta* **2006**, *259*, 2097−2100.

However, it is perhaps the magnetic behavior molecules display that is of most interest and not whether we can model them. For example, Humphrey and Wood have reported multiple areas of bistability for a Co(II) coordination polymer—without being able to explain why this bistability arises.[39] In the quest for new SMMs, preferable with higher blocking temperatures, further studies of the low-temperature dynamic behavior of the magnetization of cobalt(II) cages are required. Compound **10** would have a higher energy barrier than that of Mn_{12} *if* the slow relaxation was due to a component of the crystal which is an SMM. This illustrates a further problem—the complication provided by intermolecular interactions. Excluding these interactions and the possibility that single-chain magnets are being formed will require greater control of crystal packing than can currently be achieved.

Acknowledgment. We thank the EPSRC (U.K.) for funding for a studentship (S.L.). We are also grateful to the EC-TMR "QueMolNa" and the EC-NE "MAGMANet" for support.

Supporting Information Available: Variable-temperature magnetic behavior data of **1**, **7**, **8**, and **10**−**13** per formula unit, in PDF format. This material is available free of charge via the Internet at http://pubs.acs.org.

IC700984R

(39) Humphrey, S. M.; Wood, P. T. *J. Am. Chem. Soc.* **2004**, *126*, 13236−7.